

## Pair and single neutron transfer with Borromean $^8\text{He}$

A. Lemasson, A. Navin, M. Rejmund, N. Keeley, V. Zelevinsky, S. Bhattacharyya, A. Shrivastava, Dominique Bazin, D. Beaumel, Y. Blumenfeld, et al.

► **To cite this version:**

A. Lemasson, A. Navin, M. Rejmund, N. Keeley, V. Zelevinsky, et al.. Pair and single neutron transfer with Borromean  $^8\text{He}$ . *Physics Letters B*, Elsevier, 2011, 697, pp.454-458. 10.1016/j.physletb.2011.02.038 . in2p3-00565792

**HAL Id: in2p3-00565792**

**<http://hal.in2p3.fr/in2p3-00565792>**

Submitted on 14 Feb 2011

**HAL** is a multi-disciplinary open access archive for the deposit and dissemination of scientific research documents, whether they are published or not. The documents may come from teaching and research institutions in France or abroad, or from public or private research centers.

L'archive ouverte pluridisciplinaire **HAL**, est destinée au dépôt et à la diffusion de documents scientifiques de niveau recherche, publiés ou non, émanant des établissements d'enseignement et de recherche français ou étrangers, des laboratoires publics ou privés.

# Pair and single neutron transfer with Borromean ${}^8\text{He}$

A. Lemasson<sup>a,1</sup>, A. Navin<sup>a,\*</sup>, M. Rejmund<sup>a</sup>, N. Keeley<sup>b</sup>, V. Zelevinsky<sup>c</sup>, S. Bhattacharyya<sup>a,d</sup>, A. Shrivastava<sup>a,e</sup>, D. Bazin<sup>c</sup>, D. Beaumel<sup>f</sup>, Y. Blumenfeld<sup>f</sup>, A. Chatterjee<sup>e</sup>, D. Gupta<sup>f,2</sup>, G. de France<sup>a</sup>, B. Jacquot<sup>a</sup>, M. Labiche<sup>g</sup>, R. Lemmon<sup>g</sup>, V. Nanal<sup>h</sup>, J. Nyberg<sup>i</sup>, R. G. Pillay<sup>h</sup>, R. Raabe<sup>a,3</sup>, K. Ramachandran<sup>e</sup>, J.A. Scarpaci<sup>f</sup>, C. Schmitt<sup>a</sup>, C. Simenel<sup>j</sup>, I. Stefan<sup>a,f,4</sup>, C.N. Timis<sup>k</sup>

<sup>a</sup>GANIL, CEA/DSM - CNRS/IN2P3, Bd Henri Becquerel, BP 55027, F-14076 Caen Cedex 5, France

<sup>b</sup>Department of Nuclear Reactions, The Andrzej Soltan Institute for Nuclear Studies, ul. Hoża 69, PL-00-681 Warsaw, Poland

<sup>c</sup>NSCL and Department of Physics and Astronomy, Michigan State University, East Lansing, MI 48824, USA

<sup>d</sup>Variable Energy Cyclotron Centre, 1/AF Bidhan Nagar, Kolkata 700064, India

<sup>e</sup>Nuclear Physics Division, Bhabha Atomic Research Centre, Mumbai 400085, India

<sup>f</sup>Institut de Physique Nucléaire, IN2P3-CNRS, 91406 Orsay, France

<sup>g</sup>CRLC, Daresbury Laboratory, Daresbury, Warrington, WA4 4AD, U.K.

<sup>h</sup>Department of Nuclear and Atomic Physics, Tata Institute of Fundamental Research, Mumbai 400005, India

<sup>i</sup>Department of Physics and Astronomy, Uppsala University, Uppsala, Sweden

<sup>j</sup>IRFU/Service de Physique Nucléaire, CEA Centre de Saclay, F-91191 Gif-sur-Yvette, France

<sup>k</sup>Department of Physics, University of Surrey, Guildford, GU2 7XH, U.K.

---

## Abstract

Direct observation of the survival of  ${}^{199}\text{Au}$  residues after  $2n$  transfer in the  ${}^8\text{He}+{}^{197}\text{Au}$  system and the absence of the corresponding  ${}^{67}\text{Cu}$  in the  ${}^8\text{He}+{}^{65}\text{Cu}$  system at various energies are reported. The measurements of the surprisingly large cross sections for  ${}^{199}\text{Au}$ , coupled with the integral cross sections for the various Au residues, is used to obtain the first model-independent lower limits on the ratio of  $2n$  to  $1n$  transfer cross sections from  ${}^8\text{He}$  to a heavy target. A comparison of the transfer cross sections for  ${}^6,{}^8\text{He}$  on these targets highlights the differences in the interactions of these Borromean nuclei. These measurements for the most neutron-rich nuclei on different targets highlight the need to probe the reaction mechanism with various targets and represent an experimental advance towards understanding specific features of pairing in the dynamics of dilute nuclear systems.

**Keywords:** Borromean nucleus, Transfer reaction, Excitation function

---

The recent developments in a variety of fields like nuclei far from stability, cold atoms in traps, nanoscale condensed matter devices or quantum computing systems show how quantum-statistical and dynamic correlations between the constituents build the structure of the system. Neutron-rich radioactive nuclei, with their extended and therefore dilute matter distributions and extreme sensitivity to the precise particle number, provide unique opportunities to study the complexity and structurization of an aggregate of quantum particles [1, 2]. Light neutron-rich nuclei also carry indispensable information on properties of neutron matter. Borromean nuclei (bound three-body systems with unbound two-body subsystems), such as  ${}^6,{}^8\text{He}$  and  ${}^{11}\text{Li}$ , provide an example of binding arising essentially from

pairing correlations and therefore can be characterized as a pure embodiment of the Cooper effect [3] with one or two pairs in restricted geometry. Such structures in small composite objects are known to influence quantum tunneling [4].

Pairing correlations in small fermionic systems [5], responsible for extra binding, odd-even staggering, and modification of single-particle and collective properties, have common features with macroscopic superconductors but at the same time reveal some differences due to their mesoscopic nature. In nuclei the formally calculated coherence length of a Cooper pair is larger than the size of the nucleus, the energy gap appears on the background of a distinct shell structure, while all phase transitions are smeared. As the role of pairing correlations in nuclear structure is well known, it is of great interest to get experimental information on their dynamical aspects, especially involving Borromean nuclei. Nucleon transfer reactions, particularly on heavy targets, are an important tool for such studies [6]. The energy dependence of tunneling, related to the two-particle strength functions, probes the interaction responsible for pair formation in nuclei. The signatures of related phenomena like the nuclear (ac and

---

\*Corresponding author

Email address: navin@ganil.fr (A. Navin)

<sup>1</sup>Present address: National Superconducting Cyclotron Laboratory, Michigan State University, East Lansing, MI 48824, USA

<sup>2</sup>Permanent address: Dept. of Physics and Centre for Astroparticle Physics and Space Science, Bose Institute, Kolkata 700091, India.

<sup>3</sup>Permanent address: Instituut voor Kern- en Stralingsfysica, K.U. Leuven, Celestijnenlaan 200D, B-3001 Leuven, Belgium.

<sup>4</sup>Permanent address: Institut de Physique Nucléaire, IN2P3-CNRS, 91406 Orsay, France.

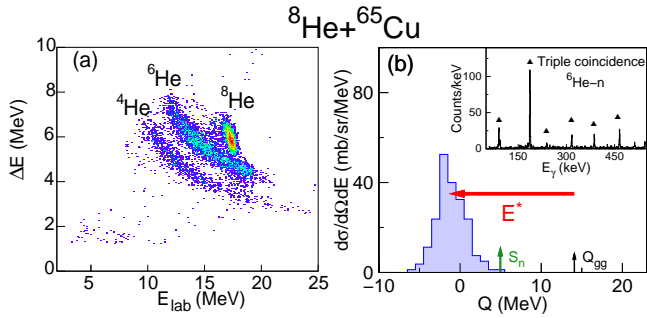


Figure 1: (color online) (a)  $\Delta E - E$  matrix for  ${}^8\text{He} + {}^{65}\text{Cu}$  at  $E_{\text{lab}} = 19.9$  MeV,  $\theta_{\text{lab}} = 35.6^\circ$ . (b)  $Q$ -value spectrum for  ${}^6\text{He}$  detected in coincidence with the 186 keV  $\gamma$  transition in  ${}^{66}\text{Cu}$ . The ground state  $Q$ -value ( $Q_{gg}$ ) for  $2n$ -stripping is shown. The  $Q$ -value spectrum was constructed assuming a binary reaction. The inset shows a triple coincidence spectrum of  $\gamma$  rays requiring the detection of  ${}^6\text{He}$  particles and neutrons (see text). Transitions in  ${}^{66}\text{Cu}$  are labeled (filled triangles).

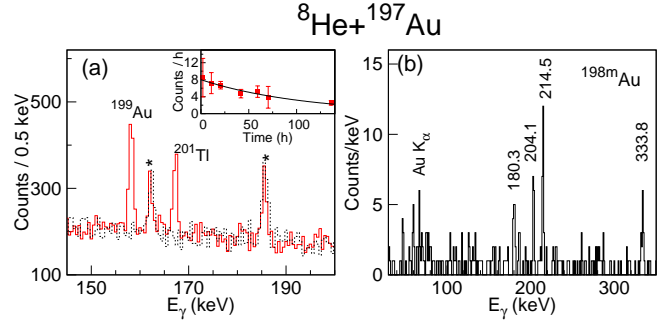


Figure 2: (color online) (a) A portion of the off-beam  $\gamma$ -ray spectrum at  $E_{\text{lab}} = 22.9$  MeV for the  ${}^8\text{He} + {}^{197}\text{Au}$  system showing the 158.4 keV  $\gamma$  ray emitted in the decay of  ${}^{199}\text{Au}$ . The corresponding background spectrum is shown by the dotted line and known transitions are denoted by asterisks.  ${}^{201}\text{Tl}$  is produced from a fusion-evaporation process. The inset shows the measured activity for  ${}^{199}\text{Au}$  fitted using the known half-life. (b)  $\gamma$ -ray spectrum obtained in coincidence with the 97 keV transition from the decay of the  $12^-$  isomeric state (811.7 keV) in  ${}^{198}\text{Au}$ .

dc) Josephson effect [7] have been discussed in recent reviews [6, 8]. Significant experimental advances [4, 9, 10, 11] in reactions using low-intensity re-accelerated radioactive ion beams (RIBs) of nuclei near the drip line, in particular for Borromean nuclei around the Coulomb barrier, have renewed hopes for observing the transfer of a single Cooper pair, “enhanced” pair transfer, and “giant pairing vibrations”. Measurements of the ratio of  $2n$ - to  $1n$ -transfer cross sections ( $\sigma_{2n}/\sigma_{1n}$ ) with Borromean nuclei are expected to be sensitive to correlations among the valence neutrons [12, 13]. The  ${}^8\text{He}$  nucleus with four loosely bound valence neutrons provides a unique system for investigating the role of neutron correlations, including pairing, in structure and dynamics of dilute nuclear systems. Additionally the work done by the Dubna group [14, 15] allow an interesting comparison to be made with the Borromean  ${}^6\text{He}$  to further highlight the role of the excess neutrons in the doubly Borromean system  ${}^8\text{He}$ .

As opposed to transfer reactions with light ions (like  $(p, t)$  or  $(p, d)$  reactions) [16], studies involving heavy ions are severely restricted by the energy resolution, so that distributions, rather than populations of discrete states, are measured. The large positive  $Q$ -values for the transfer of neutrons from light neutron-rich projectiles to heavy targets accentuate the role of neutron evaporation following transfer [17] and thus the need for exclusive measurements [10, 18]. Quasi-free scattering and transfer reactions on proton targets with  ${}^{6,8}\text{He}$  beams have been used to study the ground state properties of  ${}^8\text{He}$  [19, 20]. Both the large positive  $Q$ -values and the Borromean nature of  ${}^8\text{He}$  exclude the direct measurement of individual ( $1n$  and  $2n$ ) cross sections from the observed final residues after one- and two-neutron transfer to heavy targets, since the residues are the same in both cases. Here we show that, while in the case of  ${}^8\text{He}$  a direct measurement of  $\sigma_{2n}/\sigma_{1n}$  is not yet possible, a first and substantial step in this direction is made using an approach involving integral rather

than differential cross sections.

Measurements were performed with  ${}^8\text{He}$  beams, produced at the SPIRAL facility at GANIL, with typical intensities of  $(2 - 4) \times 10^5$  pps on  ${}^{65}\text{Cu}$  and  ${}^{197}\text{Au}$  targets, employing two independent setups using in-beam and off-beam techniques, respectively [21]. Neutron transfer reactions on  ${}^{65}\text{Cu}$  were investigated at 19.9 and 30.6 MeV using in-beam measurements of inclusive and exclusive angular distributions of light charged particles,  $\gamma$  rays and neutrons. The experimental setup consisted of 11 Compton suppressed clover HpGe detectors of the EXOGAM array and an annular Si telescope covering an angular range of  $25^\circ$ - $60^\circ$ . Fig. 1(a) shows a  $\Delta E - E$  identification plot. The observed  $\alpha$  particles arise mainly from other processes, e.g. decay of the compound nucleus. Neutrons were detected in a neutron wall consisting of 45 hexagonal detectors placed at 55 cm from the target. Further details are given in Refs. [10, 22]. Coincidences between  ${}^6\text{He}$  and  $\gamma$  rays from the transfer residue  ${}^{66}\text{Cu}$  were used to obtain the  $Q$ -distribution shown in Fig. 1(b). The peaking of the distribution around  $Q = 0$  is consistent with the semi-classical matching condition [23]. The inclusive  $Q$  distribution was found to be almost identical in shape, thus illustrating the absence of the population of bound excited states in  ${}^{67}\text{Cu}$  between  $Q_{gg}$  and  $S_n$ . The total neutron transfer cross sections,  $\sigma_{1n} + \sigma_{2n}$ , obtained from the measurement of characteristic in-beam  $\gamma$  rays of the transfer residues at 19.9 (30.6) MeV are  $782 \pm 78$  ( $759 \pm 114$ ) mb. Statistical model calculations, which fit well other evaporation residue yields [22], were used to correct for contributions arising from fusion-evaporation (The measured cross sections were corrected for contributions of 13% and 21% for the residues arising from evaporation residues at 19.9 and 30.6 MeV respectively). As expected from the large ground state  $Q$ -value of 14 MeV, population of  ${}^{67}\text{Cu}$  was not observed (upper limits of 0.5 and 1.9 mb were estimated at the two energies). To highlight the sensitivity of

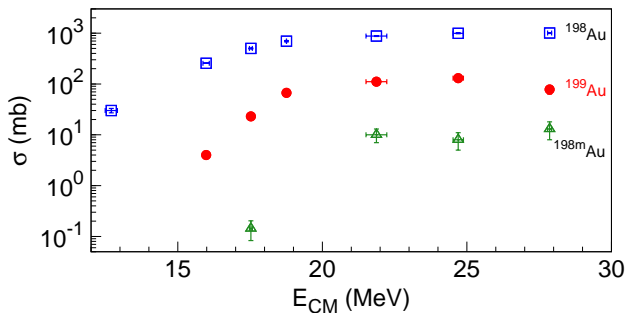


Figure 3: (color online) Cross sections for various transfer residues as a function of center-of-mass energy for the  ${}^8\text{He} + {}^{197}\text{Au}$  system.

the experimental setup, triple coincidences between  $\gamma$  rays, charged particles and neutrons (integrated over 45 detectors) measured with this low intensity beam, are shown in the inset of Fig. 1(b). Despite having the most intense  ${}^8\text{He}$  beam available today, its intensity is still lower by a factor of 200 than in the case of  ${}^6\text{He}$  [10]. This prevented building the necessary kinematic correlation of energies and emission angles between  ${}^6\text{He}$  particles and neutrons in coincidence with  $\gamma$  rays from the excited heavy residue. In addition, the decay of the unbound excited states of  ${}^6\text{He}$  to  ${}^4\text{He}$  represents an additional source of ambiguity towards the determination of individual cross sections for  $1n$  and  $2n$  transfer. Below we discuss an alternative approach.

Beams of  ${}^8\text{He}$  at energies of 18.7, 20.1 and 29.4 MeV were used to bombard stacks of two/three Au targets ( $\sim 6 \text{ mg/cm}^2$ ) separated by Al foils. After irradiation, the target and the corresponding Al foils were moved to a dedicated low-background setup and counted over a period of three weeks [4]. The  ${}^{198,198m,199}\text{Au}$  residues, formed by transfer of neutron(s) from the projectile, were identified by their characteristic  $\gamma$ -rays and half-lives [Fig. 2(a)]. Unlike the measurements with  ${}^{65}\text{Cu}$ , where  ${}^{67}\text{Cu}$  produced after  $2n$ -transfer was not observed, the corresponding residue  ${}^{199}\text{Au}$  was identified despite the large ground state  $Q$ -value of 11.96 MeV ( $> S_n$ ). Cross sections were extracted from inclusive  $\gamma$ -ray measurements and those for the  ${}^{198m}\text{Au}$  residues were obtained using  $\gamma - \gamma$  coincidences [Fig. 2(b)]. The effects of angular correlation were minimized by the close geometry of the detectors used in the experimental setup [4] and were neglected. The corrections to the transfer residues arising from the  $\alpha xn$  channels in fusion-evaporation were verified to be negligible. (Statistical model calculations that consistently reproduced the earlier measurement of the evaporation residues arising from the decay of the compound nucleus  ${}^{205}\text{Tl}$  [4] show that the contribution for  $\alpha 2n$  ( ${}^{199}\text{Au}$ ) to be less than 0.2 mb throughout the energy range of interest and those for  $\alpha 3n$  ( ${}^{198}\text{Au}$ ) to vary from 0.1 mb ( $E_{CM} = 20 \text{ MeV}$ ) to 20 mb at the highest energy measured here.) The measured integral cross sections for Au residues produced by  $1n$ - and  $2n$ -transfer in the  ${}^8\text{He} + {}^{197}\text{Au}$  system and shown

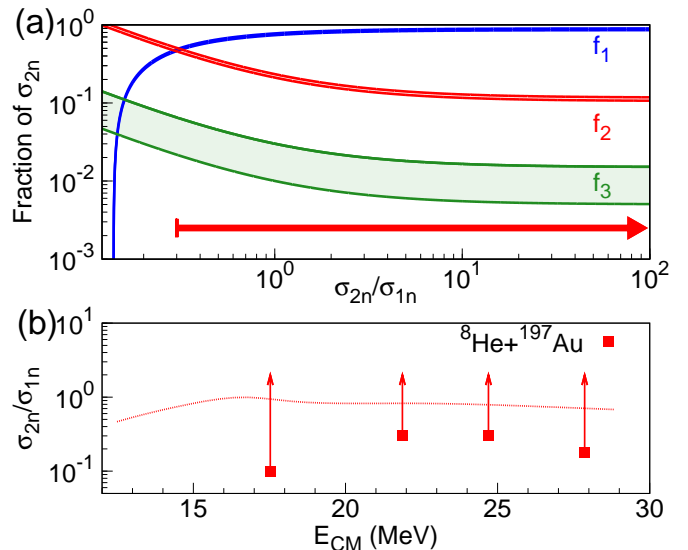


Figure 4: (color online) (a) Fractional contribution ( $f_n$ ) of  $2n$ -transfer to the observed residues as a function of  $\sigma_{2n}/\sigma_{1n}$ ;  $f_1$ ,  $f_2$  and  $f_3$  correspond to  ${}^{198}\text{Au}$ ,  ${}^{199}\text{Au}$ , and  ${}^{198m}\text{Au}$ , respectively. The curves denote solutions of Eqs. (1)-(4) using the measured cross sections at  $E_{\text{lab}} = 22.9 \text{ MeV}$ . The widths arise from the uncertainties in the measurement. The arrow indicates the allowed values for  $\sigma_{2n}/\sigma_{1n}$  (see text). (b) Lower limits on  $\sigma_{2n}/\sigma_{1n}$  (see text) and coupled-channels calculations for  ${}^8\text{He} + {}^{197}\text{Au}$ .

in Fig. 3 reveal the unexpectedly large cross section for  ${}^{199}\text{Au}$ . The measured  ${}^{198}\text{Au}$  cross sections are greater by an order of magnitude than those for  ${}^{199}\text{Au}$  and by two orders of magnitude than those for  ${}^{198m}\text{Au}$  for the whole energy range.

Making use of the fact that  ${}^{199}\text{Au}$  is observed, coupled with the measured integral cross sections for the various gold residues at a given energy, we present here for the first time a model-independent estimate of the ratio  $\sigma_{2n}/\sigma_{1n}$ . Due to the large positive  $Q$ -value for  $2n$ -transfer and the semi-classical matching condition [23], states with  $Q \simeq 0$ , i.e. at excitation energy ( $E^*$ ) in  ${}^{199}\text{Au}$  around 12 MeV, much higher than the neutron threshold ( $S_n = 7.9 \text{ MeV}$ ), are expected to be populated. Hence the measured cross sections for  ${}^{198}\text{Au}$  and  ${}^{199}\text{Au}$  *do not* correspond directly to the  $1n$ - and  $2n$ -transfer cross sections, respectively. The observed population of the  $12^-$  isomer ( ${}^{198m}\text{Au}$ ) provides direct evidence of transfer followed by evaporation since its unlikely population by  $1n$ -transfer would require a minimum  $\ell = 11\hbar$  transfer involving a  $1n_{23/2}$  neutron orbital.

The observed  ${}^{198,198m,199}\text{Au}$  cross sections represent the sum of the transfer cross section ( $\sigma_{1n} + \sigma_{2n}$ ).  $3n$ - and  $4n$ -transfer contributions (if any) are neglected. The relationships between the measured residue cross sections can be expressed as:

$$\sigma_{{}^{198}\text{Au}} + \sigma_{{}^{199}\text{Au}} + \sigma_{{}^{198m}\text{Au}} = \sigma_{1n} + \sigma_{2n} \quad (1)$$

$$\sigma_{{}^{198}\text{Au}} = \sigma_{1n} + f_1 \sigma_{2n} \quad (2)$$

$$\sigma_{{}^{199}\text{Au}} = f_2 \sigma_{2n} \quad (3)$$

$$\sigma_{{}^{198m}\text{Au}} = f_3 \sigma_{2n}, \quad (4)$$

where  $f_1$ ,  $f_2$  and  $f_3$  are the fractional contributions from  $2n$ -transfer to the observed residues of  $^{198}\text{Au}$ ,  $^{199}\text{Au}$ , and  $^{198m}\text{Au}$ , respectively ( $0 \leq f_i \leq 1$ ). These equations can be solved graphically. Fig. 4(a) represents such a solution as a function of  $\sigma_{2n}/\sigma_{1n}$  at  $E_{\text{lab}} = 22.9$  MeV. As seen from the figure, the allowed values of  $f_1$  constrain  $\sigma_{2n}/\sigma_{1n} > 0.125$ . Furthermore,  $f_3$  represents only a single state in  $^{198}\text{Au}$  populated in the statistical process of neutron evaporation, leading to the conclusion that  $f_3 \ll f_1$ . Such a limit on the allowed values of  $\sigma_{2n}/\sigma_{1n}$  is *model-independent*. The  $Q$ -distribution was assumed to peak around  $Q = 0$  similar to that measured in the case of  $^{65}\text{Cu}$  (Fig. 1(b)). Given the high excitation energy in  $^{199}\text{Au}$ , neutron evaporation is expected to be large and thus only a small fraction of states populated by  $2n$ -transfer would remain bound. This implies that  $f_1 > f_2$  and  $\sigma_{2n}/\sigma_{1n} \geq 0.3$  (Fig. 4(a)). Lower limits on the ratio at other energies are shown in Fig. 4(b) for the  $^8\text{He}+^{197}\text{Au}$  system. The above limits are the first constraints for theoretical interpretation of the role of the valence neutrons in transfer reactions with heavy targets involving  $^8\text{He}$ . Coupled-channels calculations (the details are discussed elsewhere [4]) for  $^8\text{He} + ^{197}\text{Au}$  are shown in Fig. 4(b). Due to the approximations for the spectroscopy of target-like residues in these calculations compared to those for a proton target [20, 24], the results should be taken only as a guide to qualitative understanding. More detailed calculations of the type discussed in Ref. [24] for heavy targets are necessary for a deeper theoretical analysis.

The differences in the survival of  $^{67}\text{Cu}$  and  $^{199}\text{Au}$  do not arise due to difference in center-of-mass energies with respect to the barrier. The peaking of the energy distribution around  $Q = 0$  for neutron transfer is nearly independent of the beam energy and thus so is the excitation energy. The observed differences are thus governed by the properties of target-like nuclei and can be understood in a simple manner by evaluating the fraction of bound and unbound states populated in a  $2n$ -transfer (note the analogy to the Josephson tunneling that depends on the available density of electron states). The states around  $Q = 0$  are populated, defining the range of bound and unbound orbitals available for the two neutrons. The calculations with relevant single-particle space for  $^{67}\text{Cu}$  and  $^{199}\text{Au}$  were performed using parameterized Woods-Saxon potentials [25, 26]. Combinations of the unoccupied (bound and unbound orbitals) were used to construct independent two-neutron configurations for a given spin. Assuming independent neutrons, we obtain the fractions 0.88 and 0.06 of the  $2n$  bound states in  $^{199}\text{Au}$  and  $^{67}\text{Cu}$ , respectively. The interaction between the neutrons, like pairing, causes mixing of two-neutron states increasing the number of states with an unbound component relative to the independent particle model. Using a Surface Delta Interaction (SDI) [27], with a strength parameter of  $25/A$  MeV, these fractions were found to be 0.36 and 0.06 (an upper limit, since the SDI does not mix unnatural parity states). The difference in survival of the states formed in  $^{199}\text{Au}$  and  $^{67}\text{Cu}$

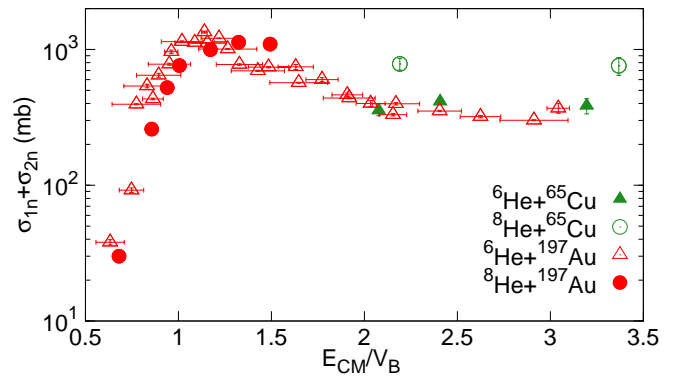


Figure 5: (color online) Measured total neutron transfer cross sections for  $^{6,8}\text{He}+^{65}\text{Cu}$  [10, 22, 28] and  $^{6,8}\text{He}+^{197}\text{Au}$  [4, 14] showing the similarities between  $^6\text{He}$  and  $^8\text{He}$ .

is found to arise due to the larger number of combinations at a similar excitation energy involving unbound single-particle orbitals in Cu as compared to those in Au. The calculations for  $^{199}\text{Au}$ , that corresponds to  $f_2$ , Eq. (3), indicate the fraction of surviving nuclei to be less than 0.36. This, in conjunction with the curve for  $f_2$  in Fig. 4(a), points to larger values of  $\sigma_{2n}/\sigma_{1n}$ , in agreement with the coupled-channel calculations shown in Fig. 4(b).

To exemplify the role of the neutron pairs in the Borromean nuclei  $^{6,8}\text{He}$ , the sum  $\sigma_{1n} + \sigma_{2n}$  is shown in Fig. 5 as a function of energy normalized to the Coulomb barrier; these excitation functions are necessary for constraining reaction models. The total transfer cross sections have a similar trend for both targets. At energies around the barrier the cross sections are comparable while above the barrier they are larger for  $^8\text{He}$ . The observed difference between  $^6\text{He}$  and  $^8\text{He}$  on both targets can be attributed to the structure of the projectile. Earlier studies on proton targets showed that  $^8\text{He}$  cannot be considered just as an inert  $\alpha$  core plus 4 neutrons; excited states of  $^6\text{He}$  are populated with significant probability [20] confirming the role of core excitations in the formation of Cooper pairs [6]; it is known [8] that pairing can be supported by coupling to the phonon-like excitations of the core, in this specific case to the  $2^+$  state in  $^6\text{He}$ . The larger cross section seen for  $^8\text{He}$  compared to  $^6\text{He}$  at higher energy may reflect a considerable difference in geometry of Cooper pairs in these isotopes. At small interaction time, the instantaneous orientation of interacting nuclei may suppress the neutron transfer from  $^6\text{He}$ , where the Cooper partners are mainly on one side of the core [29], in contrast to a more symmetric geometry of the neutron cloud in  $^8\text{He}$  [30]. Dynamics of such processes with loosely bound neutrons should be a subject of deeper theoretical studies.

A comparison of the cross sections for the transfer residues obtained for  $^6\text{He}+^{197}\text{Au}$  [14, 15] and the present work using  $^8\text{He}$  shows some interesting features. For the  $^6\text{He}+^{197}\text{Au}$  system a large cross section for the survival of the  $^{199}\text{Au}$  residue was not observed (the authors men-

tion that they determine an upper limit but do not explicitly quote an upper limit). From the data presented in Refs. [14, 15], it can be safely concluded that if this cross section was larger than around 1 mb the authors would have observed it. This low cross section is to be compared with the relatively large cross section ( $\sim 100$  mb) for the survival of  $^{199}\text{Au}$  observed in the present work. As mentioned earlier this represents only a fraction of  $2n$  transfer events. Ref. [14] also reported the measurement of the  $^{196}\text{Au}$  residue. The authors of Ref. [14] attributed the presence of  $^{196}\text{Au}$  to primarily  $-1n$  transfer but also mention other possibilities like evaporation after  $1n$  or  $2n$  transfer.  $^{196}\text{Au}$  was not observed in the present work despite the very high sensitivity of the present work using an X- $\gamma$  coincidence technique [4]. These observed differences in the interactions of these two Borromean nuclei with  $^{197}\text{Au}$  point towards how the two extra neutrons in  $^8\text{He}$  have affected the reaction mechanism despite their relative similar  $Q$ -values for the various transfer channels. The possible role of  $3n$ - and  $4n$ -channels (if any) needs to be clarified in future experiments. The usual procedure of extracting the relative dominance of the  $2n$  channel over  $1n$  by plotting the transfer probability (obtained from the differential cross section) as a function of the distance of closest approach for Coulomb trajectories [31] is not feasible with currently available RIB intensities. New experimental directions will be required to further address the problem at next-generation RIB facilities, while future reaction theory should be able to describe neutron transfers using the dynamics of their correlated wave functions in the time-dependent two-center field, a complicated analog of the Josephson effect.

In summary, we report the measurements of the cross sections for neutron transfer involving the exotic isotope  $^8\text{He}$  for various energies and different targets. A new approach used the measured integral transfer residue cross sections to set the first model-independent lower limits on  $\sigma_{2n}/\sigma_{1n}$ . These results for  $^8\text{He}$ , a system of “two Cooper pairs”, and heavy targets mark an important step in the quest to probe pairing correlations through transfer reactions compared to the use of proton targets suggested in Ref. [24]. The present work represents a major experimental step towards probing features of pairing correlations [6] using neutron rich radioactive ion beams in a dynamical regime different from that in macroscopic superconductors. Investigations to further discern the observed differences between the interaction of  $^6\text{He}$  and  $^8\text{He}$  on various targets would give a deeper insight into the understanding of interactions involving Borromean nuclei.

We thank A. Volya for providing the energies of the unbound states, P. Van Isacker, A. Vitturi and D. Lacroix for illuminating discussions. A.L. was partly supported by the Région Basse-Normandie (France). This work was supported in part by the Polish Ministry of Science and Higher Education (grant N N202 033637), NSF grant PHY-0758099 and the Swedish Research Council.

## References

- [1] D. Geesaman, et al., *Ann. Rev. Nucl. Part. Sci.* 56 (2006) 53–92.
- [2] Focus issue on open problems in nuclear structure theory, (2010). Edited by J. Dobaczewski, *J. Phys. G* 37.
- [3] L. N. Cooper, *Phys. Rev.* 104 (1956) 1189–1190.
- [4] A. Lemasson, et al., *Phys. Rev. Lett.* 103 (2009) 232701.
- [5] D. Brink, R. Broglia, *Nuclear superfluidity: pairing in finite systems*, Cambridge Univ Pr, 2005.
- [6] W. von Oertzen, A. Vitturi, *Rep. Prog. Phys.* 64 (2001) 1247–1337.
- [7] B. D. Josephson, *Phys. Lett.* 1 (1962) 251 – 253.
- [8] G. Potel, et al., preprint arXiv:0906.4298 (2009).
- [9] I. Tanihata, et al., *Phys. Rev. Lett.* 100 (2008) 192502.
- [10] A. Chatterjee, et al., *Phys. Rev. Lett.* 101 (2008) 032701.
- [11] P. A. DeYoung, et al., *Phys. Rev. C* 71 (2005) 051601.
- [12] K. Hagino, et al., *Phys. Rev. C* 77 (2008) 054317.
- [13] K. Hagino, et al., *Phys. Rev. C* 80 (2009) 031301.
- [14] Y. Penionzhkevich, et al., *Eur. Phys. J.* 31 (2007) 185 – 194.
- [15] A. A. Kulko, et al., *J. Phys. G* 34 (2007) 2297–2306.
- [16] G. Satchler, *Direct nuclear reactions*, Clarendon, 1983.
- [17] C. H. Dasso, et al., *Phys. Rev. Lett.* 73 (1994) 1907–1910.
- [18] L. Corradi, et al., *J. Phys. G* 36 (2009) 113101.
- [19] L. Chulkov, et al., *Nucl. Phys. A* 759 (2005) 43 – 63.
- [20] N. Keeley, et al., *Phys. Lett. B* 646 (2007) 222 – 226.
- [21] A. Lemasson, *Fusion et réactions directes autour de la barrière Coulombienne avec le noyau riche en neutrons  $^8\text{He}$* , Ph.D. thesis, Université de Caen Basse-Normandie, 2010. <http://tel.archives-ouvertes.fr/tel-00522577/>.
- [22] A. Lemasson, et al., *Phys. Rev. C* 82 (2010) 044617.
- [23] R. Broglia, A. Winther, *Heavy Ion Reactions*, volume 84, Addison Wesley, Redwood City, CA, 1991.
- [24] G. Potel, et al., *Phys. Rev. Lett.* 105 (2010) 172502.
- [25] N. Schwierz, et al., preprint arXiv:0709.3525 (2007).
- [26] A. Volya, Private communication (2009).
- [27] P. Brussaard, P. Glaudemans, *Shell-model Applications in Nuclear Spectroscopy*, North-Holland, 1977.
- [28] A. Navin, et al., *Phys. Rev. C* 70 (2004) 044601.
- [29] T. Neff, et al., *Nucl. Phys. A* 752 (2005) 321 – 324.
- [30] P. Mueller, et al., *Phys. Rev. Lett.* 99 (2007) 252501.
- [31] F. Funke, et al., *Z. Phys. A* 357 (1997) 303–316.